

Document downloaded from:

<http://hdl.handle.net/10251/71399>

This paper must be cited as:

Silvestre Albero, J.; Domine ., ME.; Jorda Moret, JL.; Navarro Villalba, MT.; Rey Garcia, F.; Rodriguez-Reinoso, F.; Corma Canós, A. (2015). Spectroscopic, calorimetric, and catalytic evidences of hydrophobicity on Ti-MCM-41 silylated materials for olefin epoxidations. *Applied Catalysis A: General*. 507:14-25. doi:10.1016/j.apcata.2015.09.029



The final publication is available at

<http://dx.doi.org/10.1016/j.apcata.2015.09.029>

Copyright Elsevier

Additional Information

Accepted Manuscript

Title: Spectroscopic, calorimetric, and catalytic evidences of hydrophobicity on Ti-MCM-41 silylated materials for olefin epoxidations

Author: Joaquín Silvestre-Albero Marcelo E. Domine José L. Jordá María T. Navarro Fernando Rey Francisco Rodríguez-Reinoso Avelino Corma

PII: S0926-860X(15)30162-9
DOI: <http://dx.doi.org/doi:10.1016/j.apcata.2015.09.029>
Reference: APCATA 15561

To appear in: *Applied Catalysis A: General*

Received date: 20-7-2015
Revised date: 11-9-2015
Accepted date: 21-9-2015

Please cite this article as: Joaquín Silvestre-Albero, Marcelo E. Domine, José L. Jordá, María T. Navarro, Fernando Rey, Francisco Rodríguez-Reinoso, Avelino Corma, Spectroscopic, calorimetric, and catalytic evidences of hydrophobicity on Ti-MCM-41 silylated materials for olefin epoxidations, *Applied Catalysis A, General* <http://dx.doi.org/10.1016/j.apcata.2015.09.029>

This is a PDF file of an unedited manuscript that has been accepted for publication. As a service to our customers we are providing this early version of the manuscript. The manuscript will undergo copyediting, typesetting, and review of the resulting proof before it is published in its final form. Please note that during the production process errors may be discovered which could affect the content, and all legal disclaimers that apply to the journal pertain.

**Spectroscopic, calorimetric, and catalytic evidences of hydrophobicity
on Ti-MCM-41 silylated materials for olefin epoxidations**

Joaquín Silvestre-Albero^{a,b}, Marcelo E. Domine^{a*} mdomine@itq.upv.es, José L.
Jordá^a, María T. Navarro^a, Fernando Rey^a, Francisco Rodríguez-Reinoso^b,
Avelino Corma^{a*} acorma@itq.upv.es

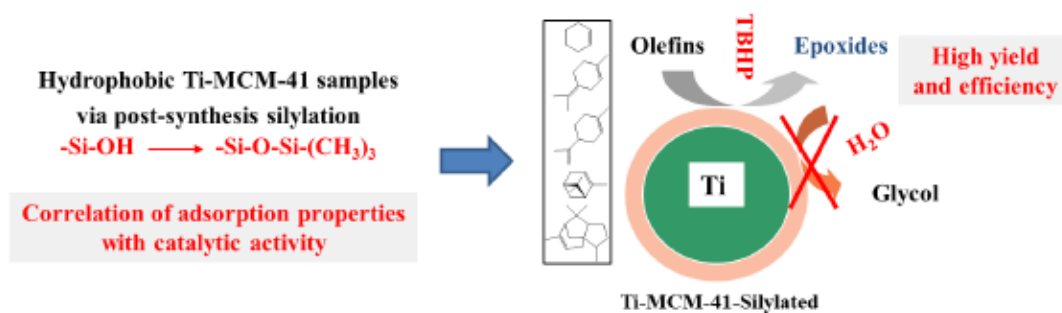
^aInstituto de Tecnología Química (UPV-CSIC). Universidad Politécnica de Valencia.
Consejo Superior de Investigaciones Científicas. Avda. Los Naranjos s/n, 46022,
Valencia, Spain

^bLaboratorio de Materiales Avanzados, Departamento de Química Inorgánica,
Universidad de Alicante, Apt. 99, E-03080, Alicante, Spain

*Tel.: +34 963879696; Fax: +34 963877809 (Marcelo E. Domine).

*Tel.: +34 963878501; Fax: +34 963877809 (Avelino Corma).

Graphical Abstract



Highlights

- Hydrophobic Ti-MCM-41-Sil. catalysts show high efficiency in olefins epoxidation with organic hydroperoxides.
- Catalytic activities are correlated with adsorption properties measured by spectroscopic techniques and calorimetry.
- Hydrophobicity level of samples is responsible for decreasing in water adsorption and catalyst deactivation by glycol poisoning.
- Increased stability of Ti-MCM-41-Sil. catalysts leads to practically quantitative production of epoxides even from natural terpenes.

Abstract

Hydrophobic Ti-MCM-41 samples prepared by post-synthesis silylation treatment demonstrate to be highly active and selective catalysts in olefins epoxidation by using organic hydroperoxides as oxidizing agents in liquid phase reaction systems. Epoxide yields show important enhancements with increased silylation degrees of the Ti-mesoporous samples. Catalytic studies are combined and correlated with spectroscopic techniques (e.g. XRD, XANES, UV-Visible, ^{29}Si MAS-NMR) and calorimetric measurements to better understand the changes in the surface chemistry of Ti-MCM-41 samples due to the post-synthesis silylation treatment and to ascertain the role of these trimethylsilyl groups incorporated in olefin epoxidation. In such manner, the effect of the organic moieties on solids, and both water and glycol molecules contents on the catalytic activity and selectivity are analyzed in detail. Results show that the hydrophobicity level of the samples is responsible for the decrease in water adsorption and, consequently, the negligible formation of the non-desired glycol during the catalytic process. Thus, catalyst deactivation by glycol poisoning of Ti active sites is greatly diminished, this increasing catalyst stability and leading to practically quantitative production of the corresponding epoxide. The extended use of these hydrophobic Ti-MCM-41 catalysts together with organic hydroperoxides for the highly efficient and selective epoxidation of natural terpenes is also exemplified.

Keywords: Hydrophobic materials, Ti-MCM-41 catalyst, Silylation treatment, Immersion calorimetry, Catalytic epoxidation.

1. Introduction

The development of ordered mesoporous materials (e.g. MCM-41 and SBA-15) has broadened the application of porous solids for processing large molecules in the fields of adsorption and catalysis [1-4]. Furthermore, the incorporation of metal species (e.g. Ti, Sn, Al, among others) to the matrix of these hexagonal ordered materials has improved their catalytic behavior on a wide range of organic reactions [5-8]. As an example, the incorporation of Ti into M41S materials (e.g. MCM-41 and MCM-48) has given rise to an improved catalytic activity and selectivity in the oxidation of bulky organic molecules when compared to recently developed microporous titanosilicates such as TS-1 and Ti-beta, where the diffusion of the reacting molecules to the active sites located inside the micropores is strongly restricted [8-11].

Among the different oxidation reactions, olefin epoxidation is of paramount importance in chemical industry, since it is used in the production of both ethylene [12] and propylene oxide [13-16], which are the raw chemicals of a myriad of end-products, such as diols and polyols. Also, the synthesis of epoxides derived from natural terpenes which are very useful as intermediates and end-products in fine chemicals industry can be successfully performed on Ti-MCM-41 catalysts [17,18]. Previous studies described in the literature have shown that the hydrophobic/hydrophilic character of the surface on these Ti-containing mesoporous materials is the most critical parameter in defining both catalytic activity and selectivity to the corresponding epoxide [19,20]. This behavior has been attributed to the competing effect of the polar epoxide reaction product with water present in the reaction mixture and the undesired diols (formed as side products through oxirane ring opening reaction) for the active sites at the surface. The hydrophobic/hydrophilic character of the siliceous framework and, consequently, the adsorption properties can be controlled by incorporation of organosilanes either in the synthesis media or by post-synthetic modification of the silanol groups. The grafted organic species decrease the concentration of silanol and Ti-OH groups on the surface, thus increasing the hydrophobic character of the synthesized material [21]. Catalytic measurements in the epoxidation of olefins have shown that silylated Ti-MCM-41 samples exhibits an improved catalytic activity and selectivity to the epoxide, the catalytic conversion being highly improved when organic hydroperoxides are used as oxidants [3, 22, 23]. Although the improved catalytic behavior on the silylated materials has been postulated to be due to their larger hydrophobicity and not to a change in the

nature of the Ti active sites, a complete physico-chemical characterization seems mandatory in order to clarify the real role of these organic functionalities.

Immersion calorimetry is a very useful technique for the surface characterization of solids. It has been widely used for the characterization of microporous solids, mainly microporous carbons [24-27]. When a solid is immersed into a non-reacting liquid there is a heat evolution called “heat of immersion” or “heat of wetting”. Commonly, this heat of immersion can provide information about the surface area available for a given molecule. However, the existence of specific interactions between the solid surface and the immersion liquid must also be taking into consideration. Accordingly, an appropriate selection of the immersion liquid can be used to characterize both the textural and/or the surface chemical properties of porous solids. In the case of silylated and non-silylated MCM-41 samples, the use of both non-polar molecules, i.e. hydrocarbons, and polar molecules such as water and alcohols, could give light in the evaluation of the hydrophobic/hydrophilic character of these synthesized materials.

With this in mind, we have combined spectroscopic techniques (e.g. XANES, UV-Visible, ^{29}Si MAS-NMR, etc.) and calorimetric measurements to better understand the changes in the surface chemistry of Ti-MCM-41 samples due to a post-synthesis silylation treatment. This information will be very useful to ascertain the role of these trimethylsilyl groups in the epoxidation of cyclohexene using *tert*-butylhydroperoxide as oxidant. The effect of the silylation degree as well as the influences of both water and diol molecules contents on the catalytic activity and selectivity will be analyzed and discussed. Examples of the extended use of these hydrophobic Ti-mesoporous catalysts together with organic hydroperoxides for the highly selective and efficient epoxidation of natural terpenes will be also provided.

2. Experimental Section

2.1. Reactants

Cyclohexene ($\geq 99.5\%$, Fluka), (1S)- α -pinene (98%, Aldrich), (R)-(+)-limonene (97%, Aldrich), terpinolene (94%, ACEDESA, S.A.), α -cedrene (99%, Fluka), *n*-nonane (99%, Aldrich), and *trans*-1,2-cyclohexane-diol (98%, Aldrich) were used as received. Acetonitrile (99.5%, Multisolvent, Scharlau), methanol (99.8%, LiChrosolv,

Merck), *tert*-butanol (99.5%, ACS, Scharlau), cyclohexane (99%, Aldrich), dichloromethane (99%, Scharlau), toluene (99%, Scharlau), and water (Milli-Q quality, Millipore) were employed without any previous treatment. For catalysts synthesis the following reactants were used: cetyl-tri-methyl-ammonium bromide (C₁₆TMAB, Aldrich), tetramethyl-ammonium hydroxide (TMAOH, 25wt% in water, Aldrich), titanium tetraethoxide [Ti(OEt)₄, TEOT, Alfa], hexamethyldisilazane [(CH₃)₃Si-NH-Si(CH₃)₃, HMDS, 97%, Aldrich], and silica (Aerosil 200, DEGUSSA). Finally, *tert*-butylhydroperoxide (TBHP, 80wt% in di-*tert*-butylperoxide/water 3/2, Fluka) was used as oxidizing agent.

2.2. Synthesis of Catalytic Materials

The Ti-MCM-41 (≈ 2.0 wt% of TiO₂) mesoporous material was prepared as reported in Refs. [19,28] starting from 3.11 g (8.53 mmol) of cetyltrimethylammonium bromide (C₁₆TAB, Aldrich) dissolved in 20.88 g (1160 mmol) of water (Milli-Q). Then, 5.39 g (14.81 mmol) of tetramethylammonium hydroxide (TMAOH, 25wt% aqueous solution, Aldrich) and 0.21 g (0.86 mmol) of titanium tetraethoxide (TEOT, Aldrich) were added to the above-mentioned solution, and the system was stirred until the titanium compound was fully dissolved. Silica (3.43 g, 56.91 mmol) was then added, giving rise to a gel having the following molar composition: SiO₂: 0.015 Ti(OEt)₄: 0.15 C₁₆TMAB: 0.26 TMAOH: 24.3 H₂O. The gel was stirred at room temperature for 1 h at 250 rpm. The resulting mixture was placed into autoclaves and heated at 373 K under autogenous pressure for 48 h. Then, the solid was recovered by filtration, washed thoroughly with distilled water, and dried at 333 K during 12 h. The solid material was placed in a tubular quartz reactor where the temperature is increased from room temperature to 813 K (under dry N₂ flow) followed by a step at 813 K during 6 h (under dry air flow). Then the solid is cooled at room temperature. The final catalyst contains 2.0 wt% (expressed as TiO₂) based on chemical analysis. This solid has a specific surface of 1090 m² · g⁻¹, with a narrow pore size distribution centred at 42.3 Å, and shows a band in the UV-Vis spectrum centred at 220 nm.

The post-synthesis silylation of Ti-MCM-41 material represented in Scheme 1 was performed as follows. Typically, 2.0 g of Ti-MCM-41 was dehydrated at 373 K and 10⁻³ Torr for 2 h. The sample was cooled at room temperature. Then, a solution of hexamethyldisilazane [(CH₃)₃Si-NH-Si(CH₃)₃, HMDS] in 30 g of toluene was added. The concentrations of HMDS solutions were adapted to attain SiMe₃/SiO₂ molar ratios

from 0 to 1. The resulting mixture was refluxed at 393 K for 90 min and washed with anhydrous toluene. The end product was dried at 333 K.

2.3. Catalyst Characterization

Phase purity of the catalysts was determined by X-ray diffraction (XRD) in a Philips X'Pert MPD diffractometer equipped with a PW3050 goniometer (CuK α radiation, graphite monochromator), provided with a variable divergence slit and working in the fixed irradiated area mode. ^{29}Si MAS NMR spectra of Ti-MCM-41 materials were recorded at a spinning rate of 5 kHz on a Varian VXR 400S WB spectrometer. Diffuse reflectance UV–Vis (DRUV) spectra of samples were recorded in a Cary 5 Varian spectrometer equipped with a “Praying Mantis” cell from Harrick.

XANES data were collected on XAS-2 station at the Laboratory for Electromagnetic Radiation Utilization (LURE) of the CNRS in Orsay (France), by using the synchrotron radiation generated by a DCI ring (1.85 GeV and 250 mA) and a double crystal Si(311) monochromator (for Ti K-edge)[29]. The spectra were measured at room temperature under He flow employing an 8 element solid-state Canberra detector for measuring the fluorescence yield. The fluorescence detection mode was used since the materials contained very low amounts of Ti (<2.0wt% as TiO $_2$). The spectra were normalized with respect to the first EXAFS oscillation (40-45 eV above the adsorption-edge). Typically, the materials were previously compacted to form self-supported wafers of \approx 100 mg, and then dehydrated at 300 °C during 2 hours. In the case of re-hydrated samples, the re-hydration treatment was carried out under air during 2 hours.

Surface area, pore volume, and pore size distribution of the solid samples (200 mg) were calculated from the nitrogen and argon adsorption isotherms at 77 and 87 K, respectively, using in a Micromeritics Flowsorb apparatus. Chemical composition was determined by atomic absorption in a Varian SpectrAA-10 Plus and elemental analysis in a Fisons EA1108CHN-S.

2.3. Immersion Calorimetry Measurements

The enthalpies of immersion of the different silylated Ti-MCM41 samples into water, methanol, *tert*-butanol, acetonitrile and cyclohexane were measured at 303 K in a Tian-Calvet type differential micro-calorimeter (Setaram, C80D). Previously to the

enthalpy measurements, the samples (100 mg) were out-gassed under vacuum into a glass bulb (10^{-5} Torr) for 3h at 373 K. After the thermal treatment the sample was sealed and transferred into the calorimeter cell. A detailed description of the experimental set-up has been previously described [27]. The areal enthalpies of immersion (mJ/m^2) have been calculated by using the BET surface area obtained from N_2 isotherms at 77 K.

2.4. Catalytic Experiments

The catalytic reactions for the cyclohexene epoxidation with *tert*-butyl hydroperoxide (TBHP) at 333 K were performed in a 25-ml round-bottom flask immersed in a thermostated bath and equipped with a condenser, a thermometer, and a magnetic stirrer. Typically, 56 mmol of the cyclohexene and 14 mmol of the oxidant (TBHP) were homogenized in the flask under stirring, and a small aliquot was taken off. Then, 30 mg of catalyst was added at once to the reaction mixture (time = 0), and the mixture was heated at reaction temperature (333 K). Thus, the olefin/TBHP ratio used was $4 \text{ mol} \cdot \text{mol}^{-1}$ and the olefin/catalyst ratio was $\approx 150 \text{ g} \cdot \text{g}^{-1}$ (0.5 wt% of catalyst referred to the olefin). When terpenes were used as substrates, experiments were carried out at 343 K during 8 h by using 8.5 mmol of terpene and 10 mmol of TBHP as oxidant (terpene/TBHP ratio = $1.17 \text{ mol} \cdot \text{mol}^{-1}$) with 150 mg of catalyst (terpene/catalyst ratio $\approx 8.0 \text{ g} \cdot \text{g}^{-1}$ (12.0 wt% of catalyst referred to the terpene). In all cases, small aliquots were withdrawn from the mixture at different time intervals to follow the kinetics of the reaction. The liquid samples were filtered off and analyzed by a 3400-Varian GC equipped with both a FID detector and a capillary column (HP-5, 30 m length), whereas identification of compounds was done by GC-MS by comparison with commercially available standards.

TBHP solution in di-*tert*-butylperoxide/water (3/2) used in this study contained around 12wt% of the di-peroxide (DTBP). It could be possible that some small amounts of di-peroxide decomposed under the reaction conditions employed here. Nevertheless, GC analysis of the reaction mixtures revealed that the DTBP amounts determined before and after the catalytic experiments were practically the same, the observed differences being insignificant; while the TBHP was drastically consumed during the process. On the basis of these results we assumed that the TBHP was the main responsible of the oxidative process taking place in the catalytic experiment.

Alkene conversion and selectivity of products are defined as [(initial moles of reactant - final moles of reactant)/ initial moles of reactant] x 100 and (moles of product

i/moles of total products) x 100, respectively. Conversion of the maximum relates to the initial moles of oxidant present in the reaction media (controlling reactant) by considering that this is equivalent to the maximum amount of alkene that can be converted (100% of conversion). TBHP efficiency is defined as: (moles of oxidation products from alkene/moles of hydroperoxide consumed) x 100.

The effect of water concentration on the catalytic activity of Ti-MCM-41 samples was studied by varying the degree of dehydration treatments performed on catalyst and reactants used in reaction. Thus, total dehydration treatments of catalyst + olefin + TBHP gives water concentration below the detection limit (Coulombimetric Karl-Fisher titration), while total dehydration of TBHP gives water concentration around 0.5 wt%. Water concentrations of 2.0 and 4.0 were attained with partial or no dehydration treatments of TBHP, respectively, whereas controlled addition of water were performed to reach water amounts in reaction media of 6.0, 8.0 and 10 wt%, respectively. In addition, the influence of the presence of *vic*-diol (glycol) on the catalytic activity of Ti-MCM-41 materials was also evaluated by adding different amounts of 1,2-cyclohexanediol (from 0.0 to 2.5 wt%) in the reaction media.

3. Results and Discussion

3.1. Physico-chemical Characterization of Ti-MCM-41 Materials

The main physical and textural properties of Ti-MCM-41 samples with different silylation degrees are summarized in Table 1. As can be seen, an increase in the C contents (from 0 to 8.9 wt%) is observed when the amount of trimethylsilyl groups anchored onto the catalytic surface increases, meanwhile the H contents on the different samples range from ca. 1wt% to 2wt%. At this point it is necessary to take into account that practically all the H contained in the Ti-MCM-41 non-silylated sample belongs to Si-OH type groups present on the solids (the ratio between Si(OSi)₄ and HO-Si(OSi)₃ is around 4 to 1, see section 3.1.2. ²⁹Si MAS-NMR spectra). In addition to this, important amounts of H₂O (until 10wt%) taken by hydration of the sample due to the humidity of the atmosphere could also be encountered on Ti-MCM-41 pristine sample. In the case of Ti-MCM-41 silylated samples, a mixture of H belonging to both Si-OH and incorporated Si-(CH₃)₃ groups are present on the solids, while the amount of H₂O

absorbed by the hydration phenomenon is strongly decreased. Replacement of H by Si-(CH₃)₃ groups occurs on the whole mesoporous material, although some non-replaced Si-OH groups remain at both the external and internal surfaces, mainly due to the steric restrictions appearing between neighbouring silanols, this taking place even at maximum level of silylation (8.9 wt% of C). In the case of C, no carbon is present on Ti-MCM-41 non-silylated sample. Thus, the C content suffered a proportional increase from 0 to 8.9 with the increasing level of Si(CH₃)₃ groups incorporation on the solids, this being taken as representative of the silylation degree of the sample. This effect is less marked in the case of H species contents, which only varied from ca. 1 to 2wt% with the increase in the silylation degree. At the same time, the initial surface area of the Ti-MCM-41 samples proportionally decreases with the incorporation of the trimethylsilyl groups onto the material (from 1090 m² · g⁻¹ on the non-silylated Ti-MCM-41[0.0] to ≈800 m² · g⁻¹ on the highly silylated Ti-MCM-41[8.9]), while pore diameter also decreases in similar way from 43 to 33 Å by passing from the non-silylated to the most silylated Ti-MCM-41[8.9] sample, respectively. This decrease in the pore diameter of around 9-10 Å is coincident with the volume occupied by the trimethylsilyl groups inside the mesopores.

Table 1.

3.1.1. X-rays diffraction analysis

Powder XRD profile of the calcined Ti-MCM41 sample shows the characteristic diffraction peaks of MCM-41 materials with reflections corresponding to (100), (110) and (200) planes, indicating a well-defined 2D hexagonal array of mesoporous channels (Fig. 1) [30,31]. Silylation of the Ti-MCM-41 sample has mainly no effect in the long-range order of the material independently of the silylation degree. In fact, the main XRD peak at a 2θ value of 2.1°, corresponding to d_{100} , does not change with the silylation degree, i.e. neither decrease in peak intensity nor shift in peak position is observed. These results show that the grafting of trimethylsilyl groups into the porous structure of Ti-MCM-41 materials exhibits no effect in the structural parameters (d spacings) of the synthesized material; changes in pore diameter of the mesopores and BET surface area upon silylation are observed and will be discussed later on.

Figure 1.

3.1.2. ^{29}Si MAS-NMR spectra

^{29}Si MAS-NMR spectra of the non-silylated sample shows two main peaks at δ -110 ppm and -100 ppm, corresponding to $\text{Si}(\text{OSi})_4$ (Q^4 species) and $\text{HO-Si}(\text{OSi})_3$ (Q^3 species), respectively (Fig. 2). Additionally, there is a weak shoulder at δ -90 ppm attributed to $(\text{HO})_2\text{Si}(\text{OSi})_2$ (Q^2 species)[31,32]. Grafting of organic functionalities into the Ti-MCM41 surface gives rise to a decrease in intensity of the Q^2 and Q^3 contributions, together with the appearance of a new resonance peak at δ 14 ppm, attributed to the silicon atoms of the trimethylsilyl group $(\text{SiO})\text{-Si}(\text{CH}_3)_3$. The intensity of this band (Q^{S} species) increases with the silylation degree. These observations clearly indicate that anchoring of the trimethylsilyl groups takes place on the free surface Si-OH species.

Figure 2.

3.1.3. UV-visible spectra

The spectra recorded by UV-Visible spectroscopy measured by diffuse reflectance (Fig. 3) show that all the Ti-MCM-41 materials present similar profiles with an unique and intense band centred around 225 nm, which can be encountered in non-silylated Ti-MCM-41 sample as well as in all the Ti-MCM-41 silylated ones. This band is assigned to isolated and tetrahedral coordinated Ti species [33,34], this fact demonstrating that the Ti environment remains unaltered and being practically not affected by the post-synthesis silylation process. Nevertheless, there is a difference in the spectrum of the non-silylated material consisting in the presence of one shoulder at approximately 270 nm, this shoulder disappearing when the degree of silylation in samples increases. This signal could be assigned to the presence of Ti species with coordination number upper than four due to the adsorption of water molecules onto these species [35]. The reduction of this shoulder with increasing silylation degree could be explained by a decrease in the interaction of water molecules with Ti atoms by an increase of the solid surface hydrophobicity due to the incorporation of trimethylsilyl groups after post-synthesis silylation treatment. Thus, water molecules are not able to coordinate to titanium, which presents a lower coordinative index remaining in a tetrahedral environment.

Figure 3.**3.1.4. X-rays adsorption spectra (XANES)**

X-rays absorption measurements close to the Ti absorption border line (XANES) were performed in order to get some spectroscopic evidence proving the above-mentioned shoulder disappearing (at 270 nm), due to the lowering on the Ti coordinative index by elimination of water molecules adsorption with increasing surface hydrophobicity by silylation treatment. As can be seen in Fig. 4, the spectra obtained for previously dehydrated non-silylated (calcined) and silylated Ti-MCM-41 materials are coincident in intensity, position, and broadness of the Ti pre-peak; this indicates that no relevant changes in the coordinative environment of Ti occurs in the absence of water. Nevertheless, important differences between calcined and silylated Ti-MCM-41 materials are observed after atmospheric moisture exposition of both previously dehydrated samples. In the case of the non-silylated material, a rapid re-hydration is observed with a drastic decrease in the relative intensity of the Ti absorption pre-peak (from 0.75 to 0.32 with respect to the first EXAFS oscillation) without changes in position and broadness (Fig. 5a). These observations are in agreement with the presence of a shoulder at 270 nm in the UV-Visible spectrum due to the presence of water molecules in the environment responsible for the increase of Ti coordinative index. In the case of the silylated material, a high hydrophobic environment in the vicinity of Ti atoms inhibits the coordination of water molecules present in atmosphere, and therefore the intensity of the Ti absorption edge in the spectrum remains unaltered (Fig. 5b). This observation is in accordance with the disappearing of the band at 270 nm observed for UV-Visible spectra of Ti-MCM-41 silylated samples.

Figure 4.**Figure 5.**

Summarizing, it can be stated that the post-synthesis silylation treatment does not disturb the Ti atoms bonding with the framework of mesoporous material. These Ti atoms are now surrounded by a strongly hydrophobic environment that inhibits the increase of the coordination number around Ti due to the presence of water molecules,

while the later molecules could easily access to the Ti sites in the non-silylated Ti-MCM-41 materials.

3.1.5. Immersion Calorimetry Measurements

A direct measurement of the hydrophobic/hydrophilic character of a material can be deduced from the enthalpy of immersion of the corresponding porous solid into liquids of different polarity (e.g. hydrocarbon vs. water). While for a non-polar molecule the total heat of immersion must be related to the total surface area available for the given molecule (due to the absence of specific interactions at the solid-liquid interface), the selection of a polar molecule (e.g. water) must give rise to an enhanced interaction at the solid-liquid interface, which can be directly related to the hydrophilic character of the material. Fig. 6 shows the areal enthalpy of immersion (mJ/m^2) for the different silylated Ti-MCM41 samples into water and cyclohexane as a function of the silylation degree. For the non-silylated Ti-MCM-41 sample the heat of immersion into water achieves a value of 125 mJ/m^2 , in close agreement with previously reported results for MCM-41 samples [36]. Interestingly, the heat of immersion into a polar molecule such as water is three times larger than that obtained with the non-polar liquid cyclohexane (46 mJ/m^2). This result confirms the presence of an important contribution of the silanol surface groups-water molecules interactions to the final heat evolved, which is in accordance with the high concentration of silanol groups and, consequently, the hydrophilic character of the MCM-41 surface. The silylation of the Ti-MCM-41 sample produces a progressive decrease in the heat of immersion for water at low coverages, this value falling drastically down to 0 mJ/m^2 for samples above a 6 wt% carbon content, which corresponds to a surface SiMe_3 coverage of 52 %. These results constitute an experimental prove of the increased hydrophobicity of Ti-MCM41 materials upon silylation. Furthermore, the progressive decay with the silylation degree at low coverage suggests a good dispersion of the silylation process, i.e. the absence of islands of SiMe_3 leaving free Si-OH groups.

Figure 6.

The absence of specific interaction between the Ti-MCM-41 surface and a non-polar molecule (cyclohexane) produces a less sensitive effect to the silylation process, the evolved heat being mainly defined by the surface area accessible. This can be

clearly seen in Fig. 6, where the areal enthalpy of immersion into cyclohexane is practically constant with the silylation degree. However, an amplification of this evolution (Fig. 6 inset) denotes certain sensitivity to the silylation process, the tendency being rather similar to that obtained with water. This result shows the existence of some specific interactions between the cyclohexane ring and the Ti-MCM-41 surface, although this effect is much more sensitive for polar molecules. Previous studies into activated carbons with different degrees of oxygen surface groups have shown a similar tendency [26].

In order to gain a better understanding of the surface chemistry, the Ti-MCM-41 samples have been studied by immersion calorimetry into a small polar molecule such as methanol (kinetic diameter = 0.43 nm), which posses a polar $-OH$ end and a non-polar $-CH_3$ terminal group (see Fig. 7). The non-silylated Ti-MCM-41 sample has an areal enthalpy of immersion of 143 mJ/m^2 . This value is $\sim 18 \text{ mJ/m}^2$ larger than that obtained with water, in accordance with the results obtained with oxidized activated carbons [26]. In fact, the $\Delta H_{\text{imm}}(\text{H}_2\text{O})/\Delta H_{\text{imm}}(\text{CH}_3\text{OH})$ ratio is 0.87 for the non-silylated Ti-MCM-41 sample, a value which is even larger than that obtained with fully oxidized activated carbons (0.68). This result provides evidences about the presence of specific interactions between the hydroxyl groups of methanol and the sylanol groups of the solid surface, characteristics of a highly hydrophilic material, as described above for water (Fig. 6). The silylation of the Ti-MCM-41 surface provides less polar surface centers and, consequently, the heat of immersion into methanol decreases. However, in contrast to the water molecule, the methanol has the possibility to rotate and interact with the surface through the non-polar methyl group. This interaction is less specific and, consequently, closer to that obtained with a hydrocarbon such as cyclohexane. This can be clearly seen in Fig. 7 where the evolution of the areal heat of immersion into methanol for the different silylated samples is shown. The enthalpy of immersion into methanol exhibits a progressive decrease with the silylation degree, this decrease being larger in the 2.5-6 wt% carbon content range, in accordance with the previous observations with water i.e. when the Si-OH surface groups are exposed. However, this heat of immersion does not fall down to 0 mJ/m^2 for highly silylated samples; an asymptotic value similar to that obtained with cyclohexane is achieved (50 mJ/m^2 for methanol vs. 36 mJ/m^2 for cyclohexane on the sample with an 8.9wt% C content).

Figure 7.

The effect of steric constrictions due to the silylation process has been studied using *tert*-butanol (2-methyl-2-propanol) as a probe molecule. Fig. 7 shows the evolution of the areal enthalpy of immersion into *tert*-butanol for the different silylated Ti-MCM41 samples. The enthalpy of immersion of the original Ti-MCM-41 sample is 120 mJ/m^2 , this value being 15% lower than that obtained with a similar alcohol such as methanol, with a smaller kinetic diameter. Assuming that in the non-silylated sample both alcohols interact preferentially through the hydroxyl group, one would expect some differences as a consequence of the steric effect due to the higher volume of the *tert*-butanol molecule. Taking into consideration a kinetic diameter of 0.43 nm for methanol and 0.60 nm for *tert*-butanol [36], the difference in the surface coverage due to steric constrictions will give rise to a decrease of 28% in the enthalpy of immersion for the larger molecule. However, the smaller difference obtained in this study between both alcohols denotes the absence of a close packing of Si-OH groups, which would give rise to a higher discrimination between both molecules. As in the case of methanol, the enthalpy of immersion decreases with the silylation degree down to an enthalpy value equal to that obtained with a hydrocarbon such as cyclohexane (36 mJ/m^2). This result reflects once again the clear differences between different polar molecules such as water and aliphatic alcohols. The presence of a non-polar end in the latest molecules provides the possibility of a re-orientation of the molecule with the evolution of the silylation process given rise to a final enthalpy value in the completely silylated sample similar to that obtained with a hydrocarbon molecule. The higher number of non-polar centers in the *tert*-butanol molecule (three $-\text{CH}_3$ groups) favors the re-orientation of the molecule at lower silylation degrees, achieving an enthalpy value close to that of cyclohexane at lower surface SiMe_3 coverages. Thus, the higher kinetic diameter of *tert*-butanol also restricts its accessibility to isolated silyanol surface groups favoring the aforementioned faster enthalpy decay.

Finally, the nature of the adsorbate-solid surface interactions has been studied by using acetonitrile (CH_3CN) as immersion molecule. Table 2 compiles the areal enthalpies of immersion into acetonitrile for the different silylated samples together with the values described previously for methanol, *tert*-butanol, water and cyclohexane. The selection of acetonitrile is based on the similar molecular size to methanol with the only change of the nature of the polar terminal group ($-\text{CN}$). For highly silylated samples, the re-orientation of the acetonitrile molecule gives rise to an interaction

through the non-polar end (-CH₃), with an enthalpy of immersion similar to that obtained with methanol or *tert*-butanol. However, for the non-silylated Ti-MCM-41 sample the heat of immersion into acetonitrile is 113 mJ/m², a value that is 20% lower than that obtained with a similar molecule, in a size basis, such as methanol. Assuming that in the non-silylated Ti-MCM-41 sample both molecules have a similar coverage and both interact through the polar end, this result denotes the important contribution of the hydroxy groups of the alcohol in the solid surface-adsorbate interaction. This is clearly demonstrated from the potential energy $\phi(z)$ equation for a given molecule at a distance z from a solid surface [31]

$$\phi(z) = \phi_D + \phi_P + \phi_{F\mu} + \phi_{FQ} + \phi_R$$

Here ϕ_P , $\phi_{F\mu}$ and ϕ_{FQ} are related with the nature of the adsorbent and the adsorptive system and these terms containing explicitly the polarizability (α) and the dipolar moment (μ) of the adsorptive molecule. Taking into consideration that both the polarizability and the dipolar moment of the acetonitrile molecule are higher than that of methanol (dipolar moment 3.84 D vs. 1.69 D for acetonitrile and methanol, respectively), the higher enthalpy of immersion for methanol into a polar surface such as MCM-41 provides a clear evidence of the presence of an additional contribution in the adsorption process i.e. the hydrogen bonding formation. This possibility of hydrogen bonding formation would be also responsible for the higher enthalpy of immersion in the case of water and *tert*-butanol.

Table 2.

3.2. Catalytic Activity of Ti-MCM-41 Materials

The catalytic activity of Ti-MCM-41 materials with different amounts of trimethylsilyl groups (different degree of silylation) was studied in the cyclohexene epoxidation with TBHP at 333 K during 5 hours and using 0.5wt% of catalyst with respect to the olefin as model reaction. As can be seen in Fig. 8, an important increase in the cyclohexene conversion as well as in the selectivity to the epoxide are observed when the Ti-MCM-41 materials are silylated by post-synthetic treatment, these augmentation being proportional to the amount of trimethylsilyl groups (wt% of C) present in the samples. Thus, an olefin conversion of 30% with epoxide selectivity

around 95% at 5 hours of reaction are obtained with Ti-MCM-41[0.0] calcined sample, conversion values being practically duplicated ($\approx 60\%$) and epoxide selectivity increased to higher than 98% when Ti-MCM-41[4.5] silylated sample is used as catalyst. Moreover, olefin conversion around 75% with epoxide selectivity close to 98% can be achieved with the most silylated Ti-MCM-41[8.9] material.

Figure 8.

In general, the low epoxide selectivity of the catalysts with low C contents (small amount of trimethylsilyl groups on surface) indicates that a fraction of the formed epoxide suffers an oxirane ring opening producing a *vic*-diol molecule (glycol), mainly due to the presence of water molecules in the vicinity of Ti active site as well as to the existence of neighbouring acid silanol groups which also could catalyze such ring opening reaction. These glycol groups formed could strongly coordinate to the Ti active sites poisoning the catalyst [19], this fact occurring at very short reaction times which justifies the low catalytic activity observed. On the contrary, high amounts of trimethylsilyl groups (high C contents) on the solid decreases the presence of acid silanol groups on the surface and, at the same time, increases the hydrophobicity of the catalyst. This diminishes the amount of water present on the catalytic surface while inhibiting the accessibility of water molecules to the Ti active sites. Thus, a much higher selectivity to the desired epoxide is reached by lowering the oxirane ring opening and, in consequence, the glycol formation. In this sense, the reduction of the amount of glycol in the reaction media as well as the own hydrophobicity of the catalyst avoiding the coordination of *vic*-diol to the Ti sites could be responsible of the high activity of Ti centres at short reaction times, but also responsible of achieving high level of olefin conversion with increasing time via inhibition of poisoning by glycol.

The effect of both silylation degree of Ti-MCM-41 materials and hydrophobicity (measured by immersion calorimetry) on olefin conversion and epoxide selectivity can be better seen in Fig. 9 (conversion values are obtained at 30 min. of reaction whereas epoxide selectivity values are taken at 25% conversion level). As can be seen, olefin conversion increases up to 10 times when comparing Ti-MCM-41[0.0] calcined sample with the most silylated Ti-MCM-41[8.9] material, this indicating that the level of poisoning by glycols is a key point that strongly depends on the degree of silylation. Thus, high catalytic activities correspond with high degrees of silylation, and similar

trends are observed when comparing the hydrophobicity of materials (Fig. 9a). However, epoxide selectivity exhibits a different behaviour with the degree of silylation of the samples. A linear correlation between the hydrophobicity of materials and selectivity to the epoxide can be encountered at C content on materials $\leq 6\text{wt}\%$, the selectivity remaining mainly constant for a higher silylation degree. These observations lead us to conclude that in order to achieve high level of epoxide selectivity the reduction of acid silanol groups is important, but the inhibition of water molecules accessibility to the actives sites is even more relevant. In fact, it is possible to reach high epoxide yields using non-silylated Ti-MCM-41 materials by only avoiding the presence of water in the reaction media [19].

Figure 9.

3.2.1. Water and Glycol Effects on the Catalytic Activity of Ti-MCM-41 Materials

Taking into account that the presence of water, and, in consequence, the formation of glycol molecules are the two more important drawbacks in olefin epoxidation reaction, the effect of different concentration of water and glycol in the catalytic activity of both non-silylated (calcined) and silylated Ti-MCM-41 materials was exhaustively studied.

In the case of water effect, the concentrations of water in reaction mixture were varied from 0 to 10 wt% by performing adequate dehydration treatments to the used catalyst, olefin, and oxidant (see section 2.4 for experimental details). As can be seen in Fig. 10a, a quite detrimental effect on catalytic activity is observed with the increase of water content in the media when Ti-MCM-41 calcined sample (non-silylated) is used as catalyst; olefin conversion and also epoxide production suffer an important decay with more than 30% lost in TON value (from 170 to 112, Fig. 10a) when the water concentration increases up to 10wt%. On the contrary, this effect is much less pronounced in the case of Ti-MCM-41 silylated material, in which the increase in water concentration up to 10% only produces a small catalytic activity decrease with a loss in TON values lower than 8% (from 989 to 915, Fig. 10a). These results also evidence the strong enhancement of catalytic activity occurring when Ti-MCM-41 silylated catalyst is used in olefin epoxidation process with TON values 6-8 times higher than those obtained with the non-silylated (calcined) sample even when appreciable amounts of water are present in reaction media. Moreover, a very low effect of water on the epoxide

selectivity is also encountered with Ti-MCM-41 silylated material as catalyst; water contents above than 8wt% are necessary to observe significant changes in olefin conversion even after 5 hours of reaction (see Fig. 11). Thus, neither the reaction rate at short reaction times (at 30 min. of reaction) nor the epoxide selectivity has significant changes by increasing the water contents in the media. These results can be explained by taking into account the high hydrophobicity of the Ti-MCM-41 silylated catalysts employed in this study, this preventing the access of water molecules to the active sites and reducing the formation of glycol molecules, and their posterior strong coordination to the Ti sites which produces final deactivation of catalyst.

Figure 10

Figure 11

In the case of glycol, the influence of 1,2-cyclohexandiol (glycol) addition was studied by varying its concentration in the reaction mixture from 0 to 2.5wt%. As can be seen in Fig. 10b and 12, the presence of glycol produces negative effects in both non-silylated (calcined) and silylated Ti-MCM-41 catalysts; the results in reaction rates (TON, mol prod · mol Ti), olefin conversion and epoxide selectivity become worse in the case of the Ti-MCM-41 calcined sample. Thus, glycol contents of 1 wt% in reaction media, which could be easily and commonly found in epoxidation reactions, strongly decrease catalytic activity of Ti-MCM-41 calcined sample with more than 85% loss in TON value (from 170 to 21, Fig. 10b). Reaction rate (at 30 min. of reaction) was also reduced by glycol addition in the case of Ti-MCM-41 silylated catalyst, although the activity decay (TON lost c.a. 20%) as less detrimental for this sample by showing a TON value of 765 (Fig. 10b). Moreover, the presence of small amounts of glycol also leads to a decrease in olefin conversion from $\approx 100\%$ to around 87% after 5 hours of reaction with Ti-MCM-41 silylated catalyst (Fig. 12). All these observations indicate the rapid and non-reversible adsorption of glycol molecules on the Ti active sites of the solid. In this case, although the catalyst presents a high hydrophobic surface, this is not enough to prevent the poisoning of metallic center when high amounts of glycol are present in the reaction media.

Figure 12.

Summarizing, it is possible to conclude that glycol is the more important deactivating agent of those that could be, for instance, present in this type of olefin epoxidations, the preparation of high hydrophobic Ti-MCM-41 catalyst by post-synthesis silylation treatment being crucial to preserve the catalytic activity. In such way, the coordination of water molecules to the active sites is inhibited, and, indirectly, the production of glycol molecules by the epoxide ring opening is avoided. However, in order to achieve a much higher catalytic activity, efficiency, and stability during reaction time of the Ti-MCM-41 silylated materials, even in the presence of high concentration of glycol in the media, it is possible to incorporate other metal sites able to trap the molecules of glycol formed during reaction. One solution that could be suggested consists in the increase of the amount of Ti included in the catalyst generating an extra-amount of Ti sites, some of them being sacrificed as glycol traps and preserving the rest of Ti active sites in the catalyst for olefin epoxidation takes place.

3.2.2. Terpene Epoxidations with TBHP using Ti-MCM-41 Silylated Materials

After the very high olefin conversion and excellent epoxide selectivity (>99%) attained with the high hydrophobic Ti-MCM-41 silylated material in the cyclohexene epoxidation with TBHP, the scope of this Ti-mesoporous catalyst was extended to the epoxidation of other interesting olefin compounds (i.e. terpenes) always working with organic hydroperoxides as oxidizing agents. Thus, different terpenic structures were selected as substrates to carry out the selective catalytic epoxidation with TBHP at 343 K during 8 hours by using a TBHP / terpene molar ratio of 1.2 with 10-12wt% of Ti catalysts (150 mg) with respect to the terpene (see 2.4 section for experimental details).

The results of terpinolene, limonene, α -pinene, and α -cedrene selective epoxidation with TBHP using both calcined (non-silylated) and silylated Ti-MCM-41 materials are shown in Table 3. In all the cases, the Ti-MCM-41 catalysts demonstrates their capacity to oxidize the different terpenic substrates, even the more voluminous such as the α -cedrene, while comparison between the calcined and the silylated Ti-MCM-41 samples clearly evidences the higher catalytic performance of the optimized hydrophobic material.

It is Worthing to note that the epoxidation reactions of these terpenic compounds are much more demanding processes compared with the cyclohexene epoxidation because the terpene oxides formed are quite reactive under reaction conditions, the

corresponding oxirane ring opening being much faster than the observed in the case of 1,2-epoxy-cyclohexane. As a matter of fact, this epoxide ring opening in terpenes produces the formation of glycols with the well known deactivation of catalyst by coordination of those glycol molecules onto the Ti active sites. Moreover, other sub-products are also formed by re-ordination of the terpenic structures after oxirane ring opening, this fact troubling even more reaching high yield of the desired epoxide. The amounts of all these sub-products together with the glycols formed are reported for each corresponding terpene as “Others” in Table 3.

Table 3.

The relevance of the post-synthesis silylation treatment and the corresponding increase in hydrophobicity of catalyst surface can be observed by comparing the catalytic activity achieved with the non-silylated and silylated Ti-MCM-41 samples (Table 3). As can be seen, epoxide yields obtained for each one of the tested terpenes are significantly superior with the Ti-MCM-41 silylated catalysts than those referred to the Ti-MCM-41[0.0] calcined sample. Thus, in the case of α -pinene conversion increases from 10 to 85% by using the silylated material instead of the calcined one, while the epoxide selectivity (78%) observed with the former catalyst is practically 10 times higher than the selectivity value (8%) achieved with the Ti-MCM-41 calcined material. At the same time, it is very important to remark that TBHP efficiency is also enhanced for all the terpenes studied in a similar way when the highly hydrophobic Ti-catalyst is used instead of the non-silylated material. Thus, TBHP efficiencies close to 100% are attained with Ti-MCM-41 silylated catalyst using α -pinene as substrate.

Interestingly, all these results obtained with terpenic substrates can be enhanced by optimising reaction conditions for each special terpene in function of its structure and functionality, this extending the application of this hydrophobic Ti-MCM-41 silylated catalyst to a broad range of olefin compounds.

4. Conclusions

The enhancement of catalytic activity and the decrease in deactivation during olefin epoxidation due to the increase of hydrophobic properties of Ti-MCM-41 catalyst by incorporation of trimethylsilyl groups after post-synthesis silylation treatment have been demonstrated here through a combinative study including spectroscopic evidences, calorimetric measurements, and catalytic data.

The most interesting effect observed is an important decrease in the amount of water adsorbed on the Ti-mesoporous materials by increasing the hydrophobicity of the samples, as can be observed from immersion calorimetric data by using water as probe molecule. UV-Visible spectra measured by diffuse reflectance also confirm this behaviour showing that the signal (shoulder at $\approx 270\text{nm}$) assigned to Ti species coordinated with water adsorbed molecules in Ti-MCM-41 calcined (non-silylated) sample practically disappears with increasing silylation degree of Ti-MCM-41 materials. These observations are in agreement with X-ray adsorption measurements (XANES) evidencing that water molecules have a great tendency to coordinate with Ti atoms bonded with MCM-41 framework in non-silylated samples, thus forming Ti hydrated species with coordination number higher than four. Nevertheless, only tetrahedrally coordinated Ti atoms appear in Ti-MCM-41 silylated sample even in the presence of water because Ti atoms are surrounded by a strong hydrophobic environment, thus avoiding water molecules to access onto those sites. Increase in silylation degree on Ti-mesoporous samples also correlates with the reduction of Q^2 $[(\text{HO})_2\text{Si}(\text{OSi})_2]$ and Q^3 $[\text{HO}-\text{Si}(\text{OSi})_3]$ species peaks observed by ^{29}Si MAS-NMR spectroscopy together with the slightly growing of the Q^4 $\text{Si}(\text{OSi})_4$ signal and the appearance of a new resonance peak Q^S $[(\text{SiO})-\text{Si}- (\text{CH}_3)_3]$ at $\delta=14\text{ppm}$ corresponding to trimethylsilyl groups anchored onto the free surface Si-OH species, the intensity of later peak increasing with the amount of organic groups incorporated on solid.

All the above-mentioned spectroscopic evidences prove the significance of silylation degree in Ti-MCM-41 samples, but, more interestingly, their catalytic activity is linearly related to the hydrophobicity level of the materials expressed as the areal enthalpy of immersion (ΔH , mJ/m^2) in water and measured by calorimetric experiments. As a consequence, increasing the hydrophobic character of Ti-MCM-41 catalyst decreases and prevents water adsorption on Ti active sites. The absence of water in the environments of Ti sites improves epoxide formation and stability by inhibiting (or at least reducing in large extent) the oxirane ring opening reaction that could be suffered by the epoxide during the olefin epoxidation process to produce the corresponding

glycol. As demonstrated here, glycol is irreversibly adsorbed onto Ti active sites and its formation is the main responsible of catalytic deactivation in the epoxidation process. In this sense, the silylation treatment on Ti-MCM-41 material avoids glycol generation, thus favouring the catalyst stability and life during oxidation process.

In conclusion, it has been proven that highly hydrophobic Ti-MCM-41 samples possess an elevated catalytic activity in the selective epoxidation of olefins and terpenes by using organic hydroperoxides as oxidizing agents in liquid phase reaction systems. The high hydrophobicity of the samples is responsible for the decrease in water adsorption and the negligible formation of the non-desired glycol during the process, thus conducting to practically quantitative production of the corresponding epoxide.

Acknowledgements

The authors gratefully acknowledge financial support of Spanish Government (MAT2012-38567-C02-01, Consolider-Ingenio 2010-Multicat CSD-2009-00050 and Severo Ochoa SEV-2012-0267) and Generalitat Valenciana (Project Prometeo). M.E.D. also thanks funds from Spanish Government (CTQ-2011-27550) and CSIC (PIE 200980I063). J.S.A. and F.R.R. acknowledge financial support from MINECO (Projects MAT2013-45008-p and CONCERT Project-NASEMS (PCIN-2013-057), and from Generalitat Valenciana (PROMETEO2009/002).

References

1. C. T. Kresge, M. E. Leonowicz, W. J. Roth, J. C. Vartuli, J. S. Beck, *Nature* 359 (1992) 710.
2. D. Zhao, J. Feng, Q. Huo, N. Melosh, G. H. Fredrickson, B. F. Chmelka, G. D. Stucky, *Science* 279 (1998) 548.
3. A. Corma, *Chem. Rev.* 97 (1997) 2373.
4. A. Taguchi, F. Schuth, *Microp. Mesop. Mater.* 77 (2005) 1.
5. A. Corma, M. T. Navarro, L. Nemeth, M. Renz, *Chem. Commun.* (2001) 2190.
6. A. Corma, M. T. Navarro, J. Pérez-Pariente, F. Sánchez, *Stud. Surf. Sci. Catal.* 84 (1995) 69.
7. T. J. Pinnavaia, W. Zhang, *Stud. Surf. Sci. Catal.* 117 (1998) 23.

8. S. Gontier, A. Tuel, *J. Catal.* 157 (1995) 124-132.
9. A. Corma, M. T. Navarro, J. Pérez-Pariente, *J. Chem. Soc., Chem. Commun.* (1994) 147.
10. P. T. Tanev, M. Chibwe, T. J. Pinnavaia, *Nature* 368 (1994) 321.
11. K. A. Koyano, T. Tatsumi, *Chem. Commun.* (1996) 145.
12. T. E. Lefort (Soc. Fr. Cat. Gén.), FR Patent 729 952, 1931; FR Patent 771 650, 1934; and US Patent 1 998 878, 1935.
13. J. P. Schmidt, US Patent 3 988 353, 1976, to Oxirane Co.
14. F. Wattimena, H. P. Wulff, GB Patent 1 249 079, 1971, to Shell Oil Co.
15. J. Tsuji, J. Yamamoto, A. Corma, F. Rey, US Patent 6 211 388, 1998, assigned to Sumitomo Chemical Company, Ltd.
16. M. T. Navarro, A. Corma, J. L. Jorda, F. Rey, WO 2000007710 A2, 2000.
17. W. F. Hölderich, G. Heitmann, *Catal. Today* 38 (1997) 227.
18. A. Corma, S. Iborra, A. Velty, *Chem. Rev.* 107 (2007) 2411.
19. A. Corma, M. Domine, J. A. Gaona, J. L. Jorda, M. T. Navarro, F. Rey, J. Pérez-Pariente, J. Tsuji, B. McCulloch, L. T. Nemeth, *Chem. Commun.* (1998) 2211.
20. A. Corma, M. E. Domine, M. Susarte, F. Rey, WO 2000054880 A1, 2000.
21. E. Gianotti, V. DellaRocca, M. L. Peña, F. Rey, A. Corma, S. Coluccia, L. Marchese, *Res. Chem. Intermed.* 30(9) (2004) 871.
22. T. Tatsumi, K. A. Koyano, N. Igarashi, *Chem. Commun.* (1998) 325.
23. T. Blasco, A. Corma, M. T. Navarro, J. Pérez-Pariente, *J. Catal.* 156 (1995) 65.
24. R. Denoyel, J. Fernández-Colinas, Y. Grillet, J. Rouquerol, *Langmuir* 9 (1993) 515.
25. H. F. Stoeckli, *Carbon* 28 (1985) 1.
26. F. Rodríguez-Reinoso, M. Molina-Sabio, M. T. Gonzalez, *Langmuir* 13 (1997) 2354.
27. J. Silvestre-Albero, C. Gómez de Salazar, A. Sepúlveda-Escribano, F. Rodríguez-Reinoso, *Colloids and Surfaces A* 187-188 (2001) 151.
28. A. Corma, J. L. Jordá, M. T. Navarro, J. Pérez-Pariente, F. Rey, J. Tsuji, *Stud. Surf. Sci. Catal.* 129 (2000) 169.
29. F. Rey, G. Sankar, T. Maschmeyer, J. M. Thomas, R. G. Bell, G. N. Greaves, *Top. Catal.* 3 (1996) 121.
30. J. S. Beck, C. T.-U. Chu, Y. Johnson, C. T. Kresge, M. E. Leonowicz, W. Roth, J. C. Vartuli, WO 11390/1991, 1991.

31. J. S. Beck, J. C. Vartuli, W. J. Roth, M. E. Leonowicz, C. T. Kresge, K. D. Schmitt, C. T.-U. Chu, D. H. Olson, E. W. Sheppard, S. B. McCullen, J. B. Higgins, J. L. Schlenker, *J. Am. Chem. Soc.* 114 (1992) 10834.
32. C.-Y. Chen, H. X. Li, M. E. Davis, *Microporous Mater.* 2 (1993) 27.
33. S. Coluccia, L. Marchese, G. Martra, *Microp. Mesop. Mater.* 30 (19 (1999) 43.
34. V. Bolis, S. Bordiga, C. Lamberti, A. Zecchina, A. Catari, F. Rivetti, G. Spanò, G. Petrini, *Microp. Mesop. Mater.* 30 (1) (1999) 67.
35. F. Geobaldo, S. Bordiga, A. Zecchina, E. Giamello, G. Leofanti, G. Petrini, *Catal. Lett.* 16 (1992) 109.
36. M. J. Meziani, J. Zajac, J.-M. Douillard, D. J. Jones, S. Partyka, J. Roziere, *J. Colloid and Interf. Sci.* 233 (2001) 219.
37. S. J. Gregg, K. S. W. Sing, *Adsorption, Surface Area and Porosity*. 2nd Edition, Academic Press, London, UK, 1982, 303 pp.

Figure Captions

Figure 1: X-rays diffractograms of Ti-MCM-41 materials with different silylation degrees.

Figure 2: ^{29}Si NMR MAS spectra of Ti-MCM-41 materials with different silylation degrees.

Figure 3: Diffuse reflectance UV-Visible spectra of Ti-MCM-41 materials with different silylation degrees.

Figure 4: X-rays absorption (XANES) spectra of dehydrated Ti-MCM-41 calcined and silylated materials.

Figure 5: X-rays absorption (XANES) spectra of dehydrated and rehydrated Ti-MCM-41 materials, (a) calcined, and (b) silylated.

Figure 6: Evolution of the areal enthalpies of immersion (mJ/m^2) in water (H_2O) and cyclohexane (C_6H_{12}) as a function of carbon content for the different silylated Ti-MCM-41 samples.

Figure 7: Evolution of the areal enthalpy of immersion (mJ/m^2) in methanol and 2-methyl-2-propanol as a function of carbon content for the different silylated Ti-MCM-41 samples.

Figure 8: Catalytic activity of Ti-MCM-41 materials with different silylation degrees in the cyclohexene epoxidation with TBHP (and 0.5 wt% of catalyst) at 333 K during 5 h. (a) Cyclohexene Conversion (%Mol.); (b) Epoxide Selectivity (%Mol.).

Figure 9: Changes in catalytic activity (a) and epoxide selectivity (b) in the cyclohexene epoxidation with TBHP (at 333 K during 5 h.) of Ti-MCM-41 materials with different silylation degrees in function of the hydrophobicity level.

Figure 10: Effect of water (a) and vic-diol (1,2-cyclohexanediol) (b) concentrations on the catalytic activity (TON, mol prod · mol of Ti) of Ti-MCM-41 calcined and silylated materials in the cyclohexene epoxidation with TBHP (at 333 K) at 30 min. of reaction.

Figure 11: Effect of water concentration on the epoxide selectivity in the cyclohexene epoxidation with TBHP (at 333 K) of Ti-MCM-41 silylated material at 30 min. (a), and 5 h (b) of reaction.

Figure 12: Effect of vic-diol (1,2-cyclohexanediol) concentration on the epoxide selectivity in the cyclohexene epoxidation with TBHP (at 333 K) of Ti-MCM-41 silylated material at 30 min. (a), and 5 h (b) of reaction.

Scheme 1: Representation of the post-synthesis silylation treatment of Ti-MCM-41 sample.

Figure 1:

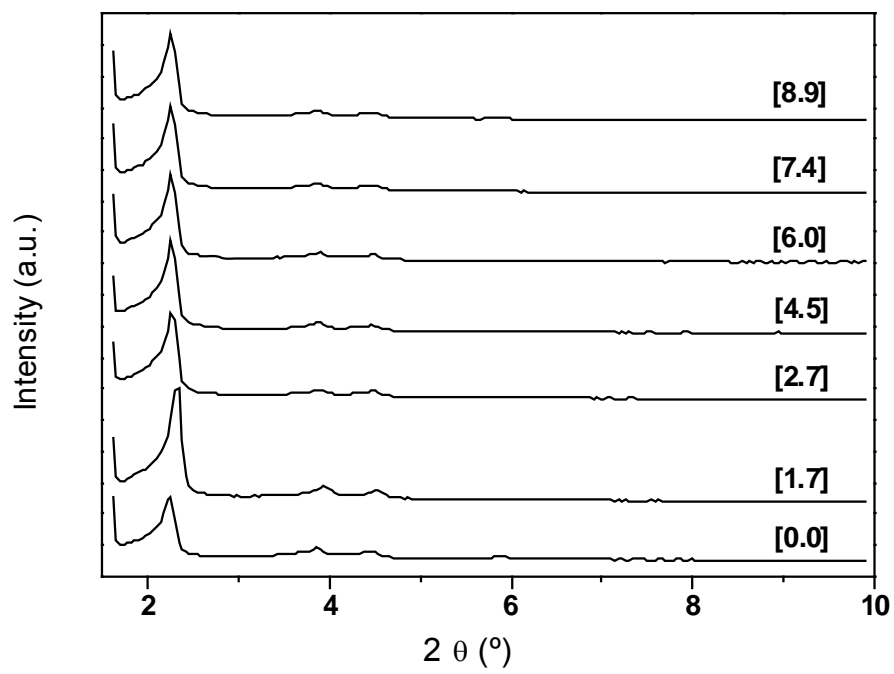


Figure 2:

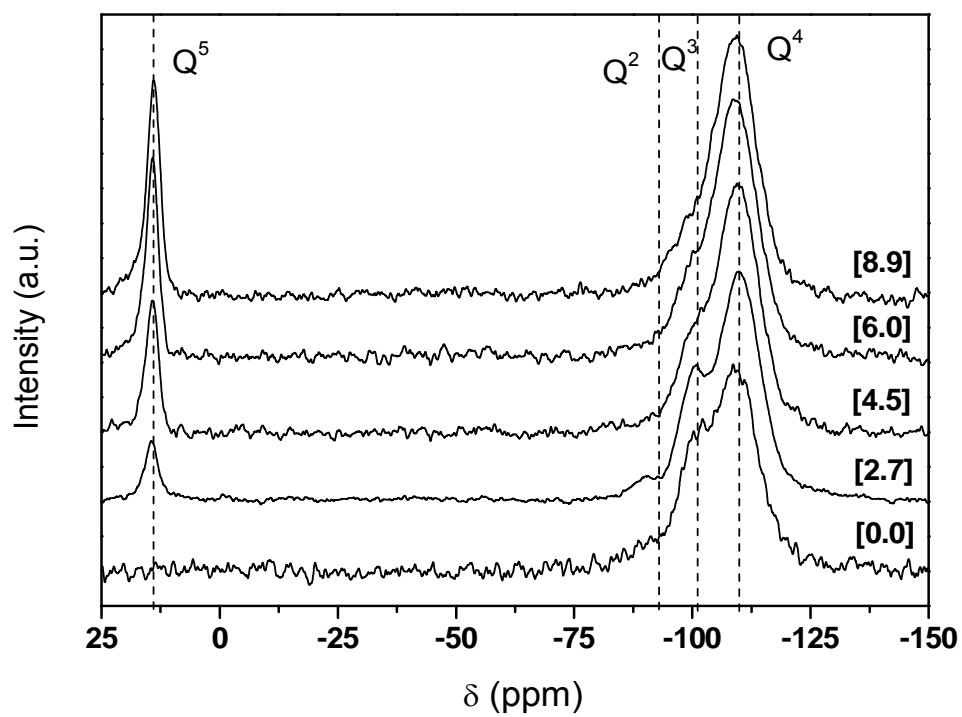


Figure 3:

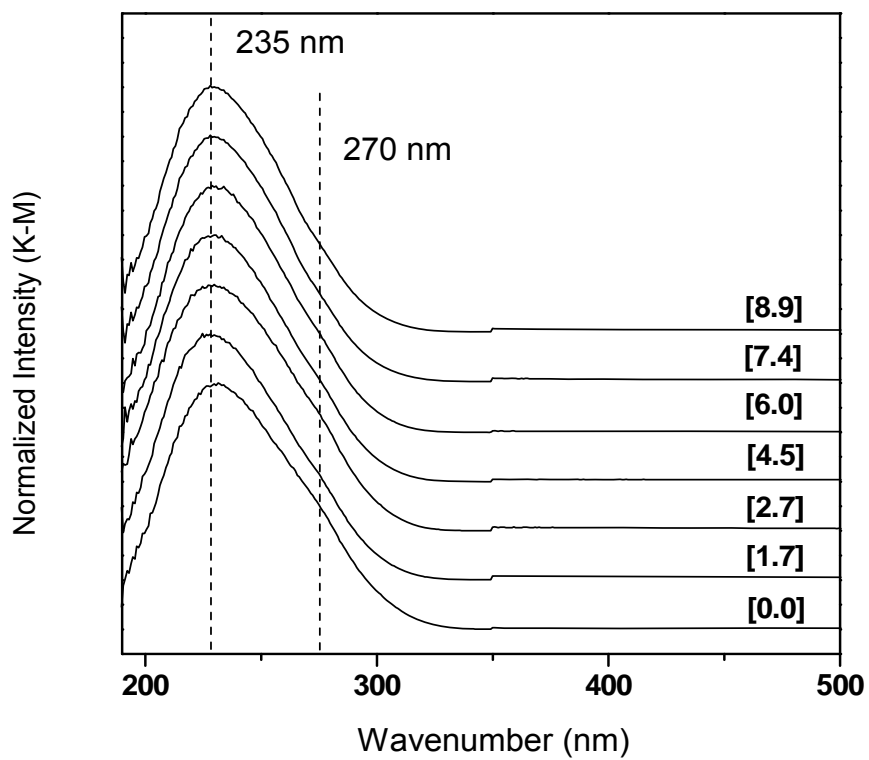


Figure 4:

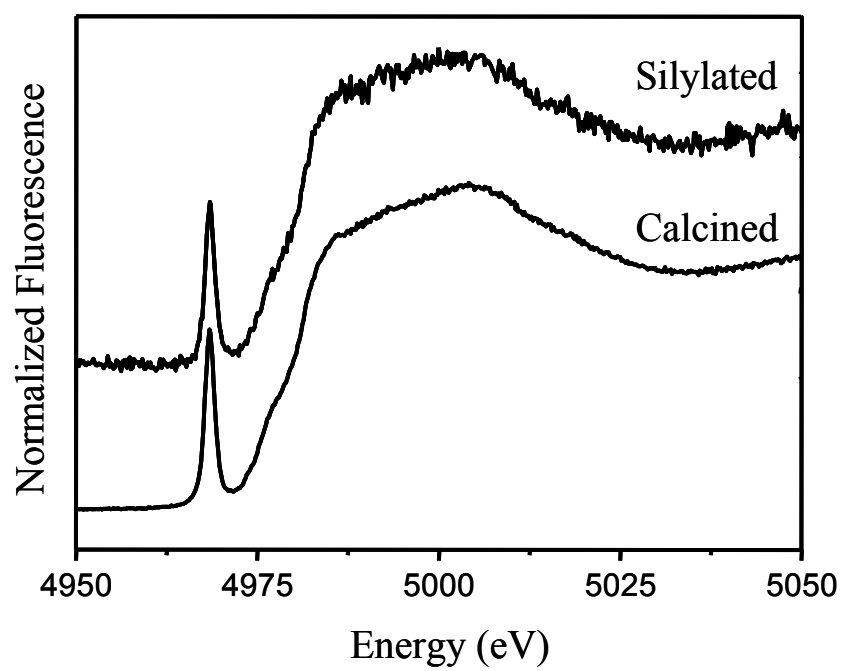


Figure 5:

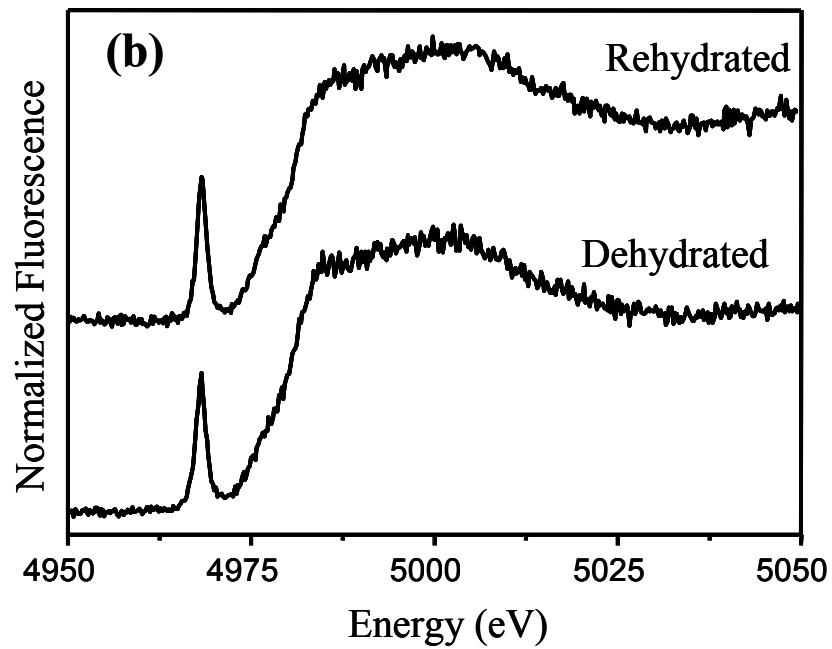
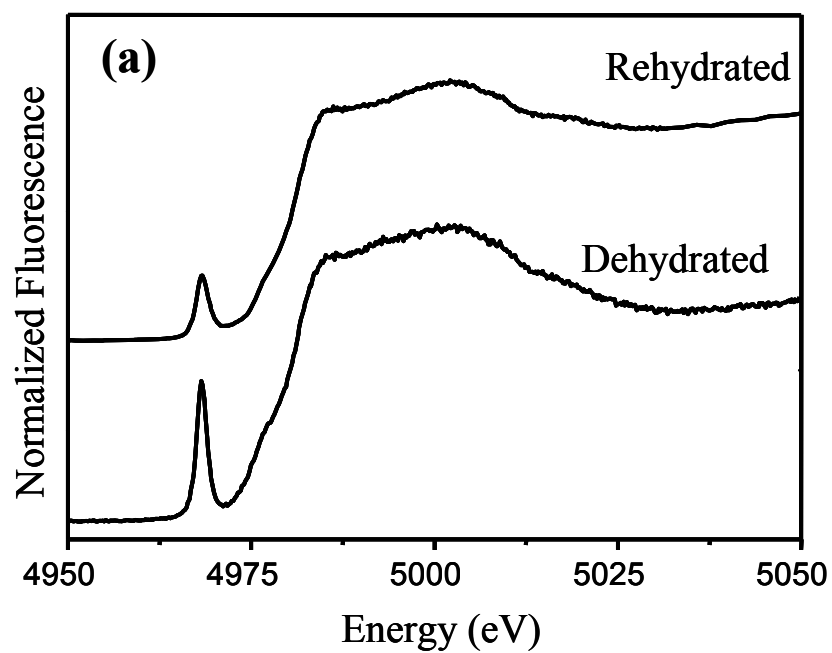
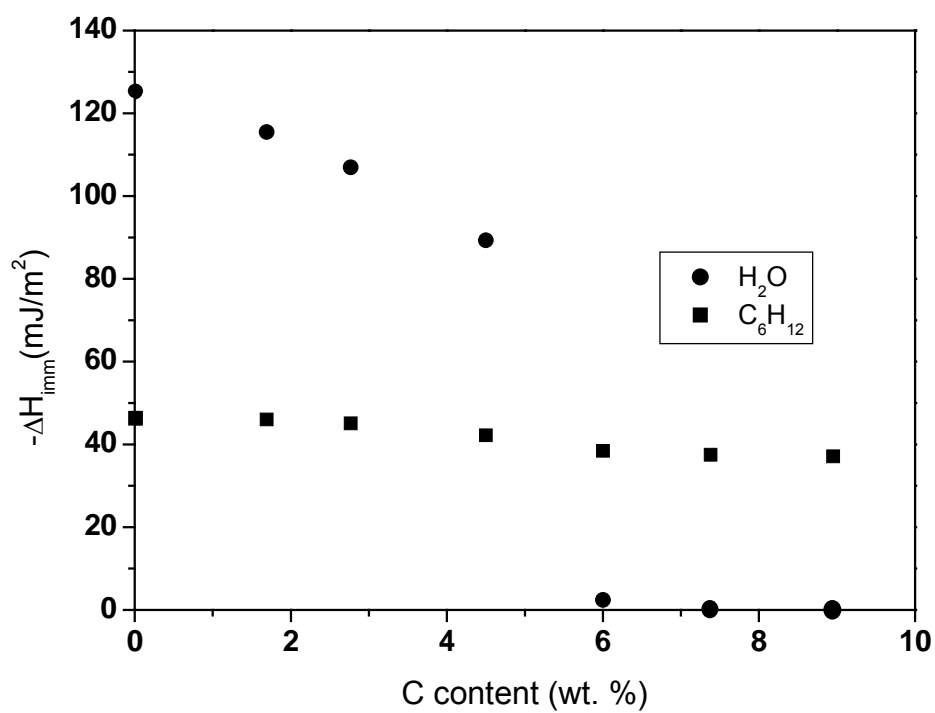


Figure 6:



Appendix Figure 6

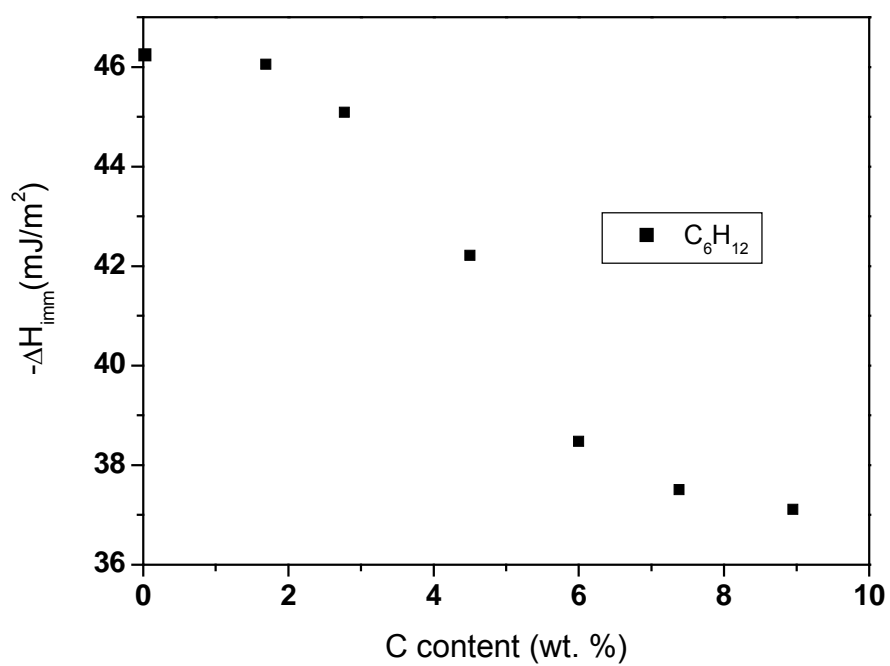


Figure 7:

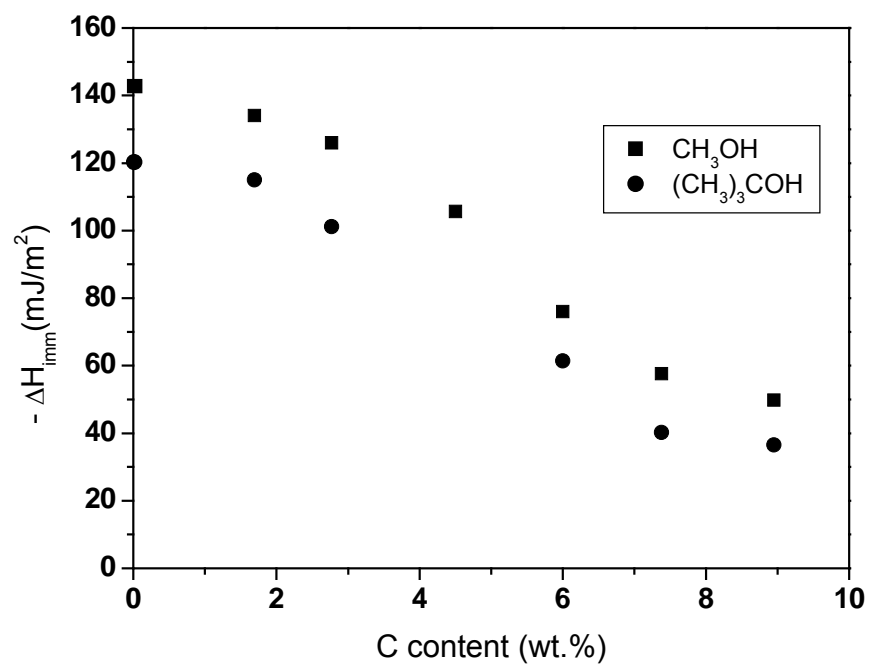


Figure 8:

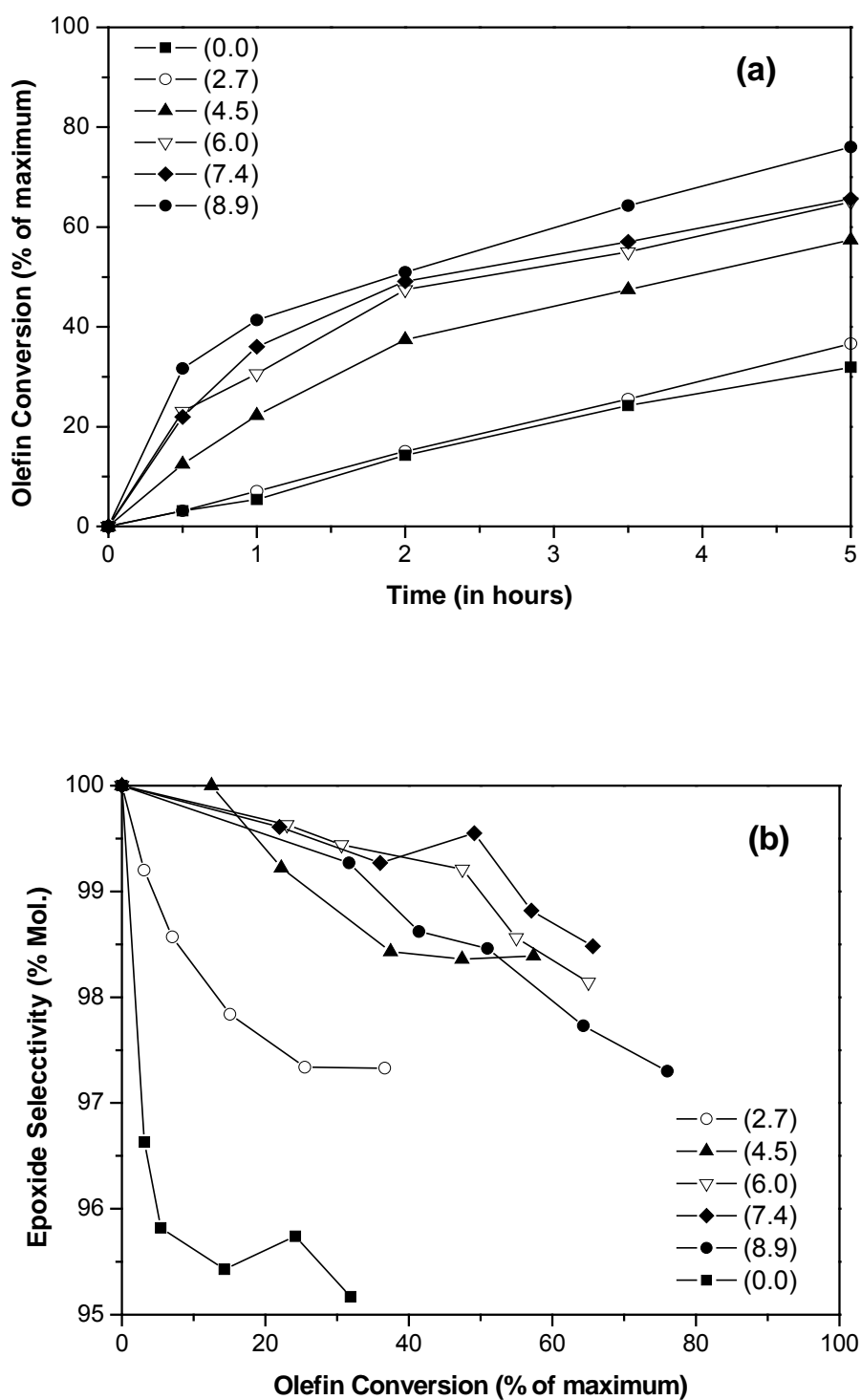


Figure 9:

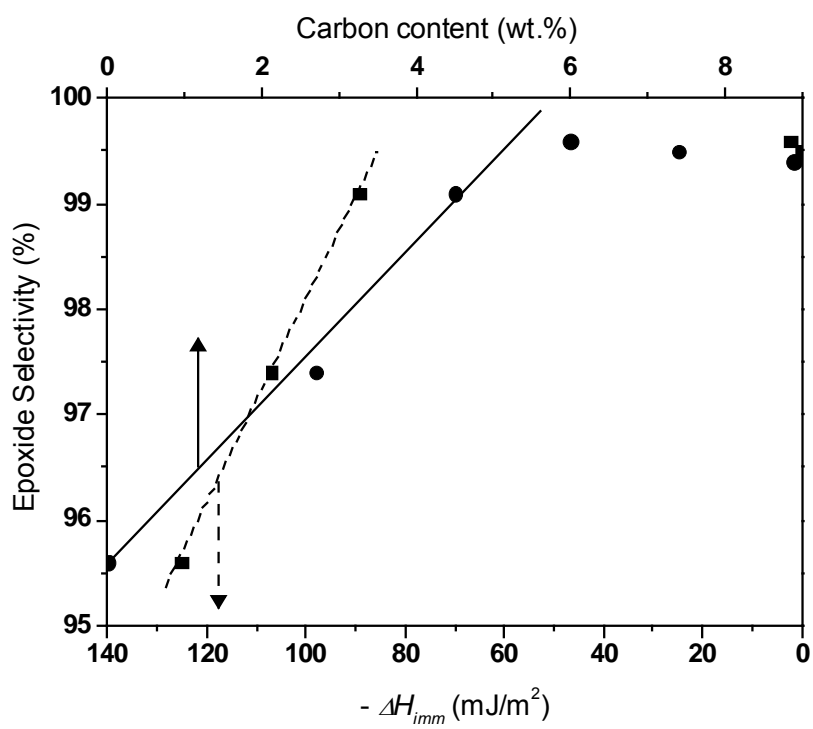
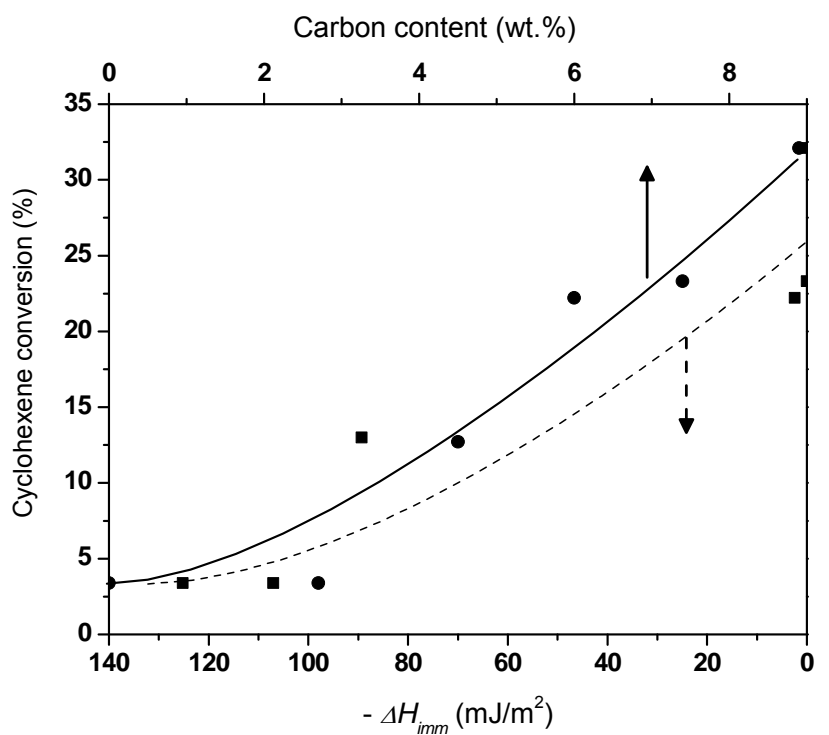


Figure 10:

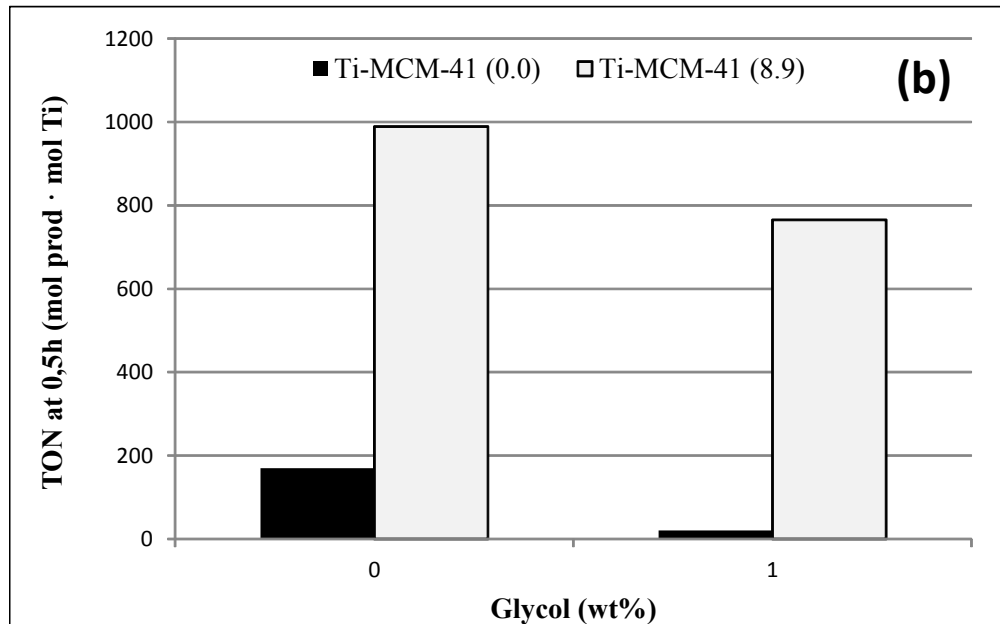
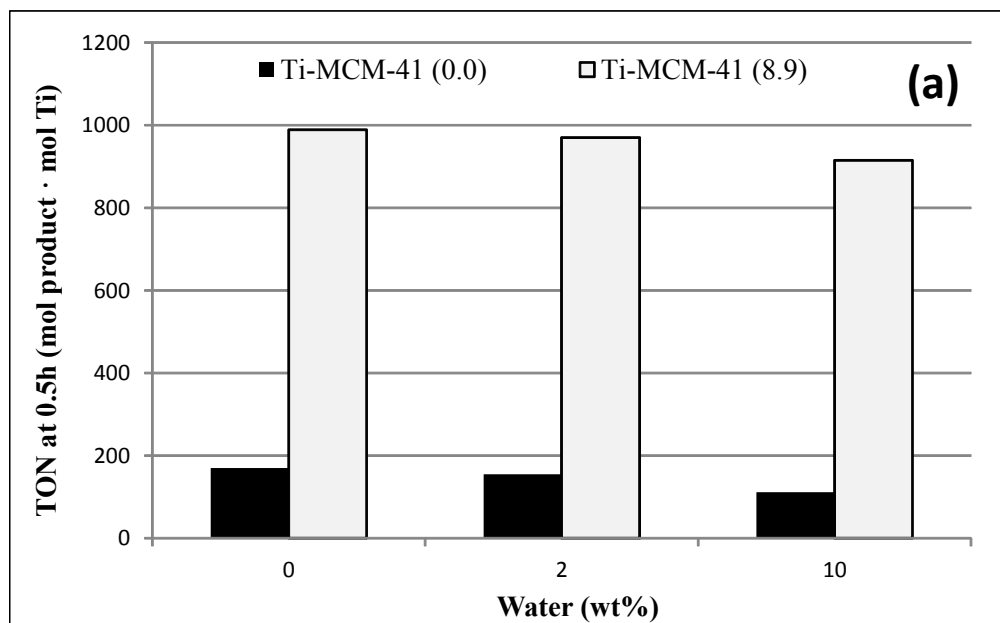


Figure 11:

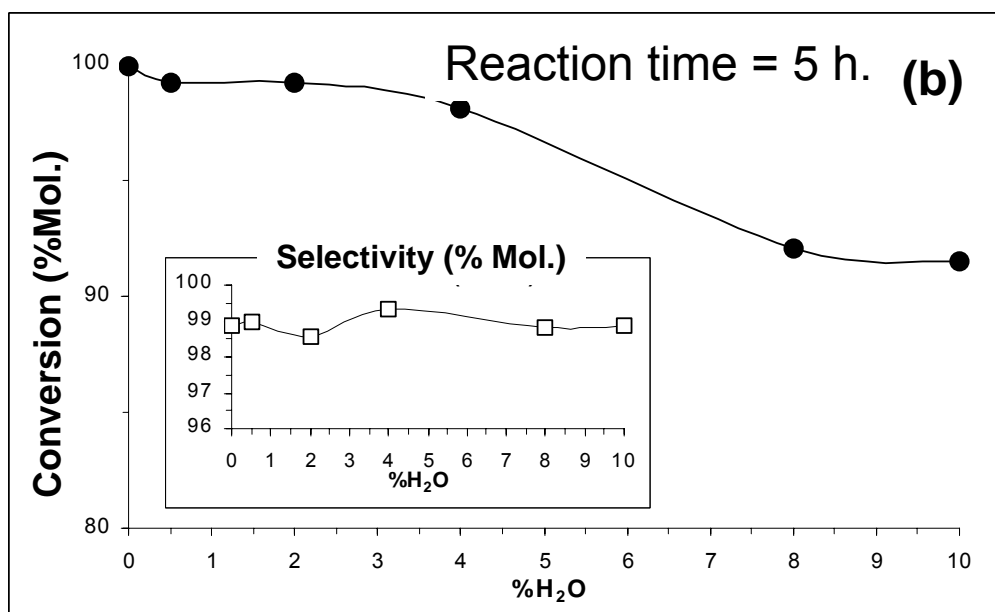
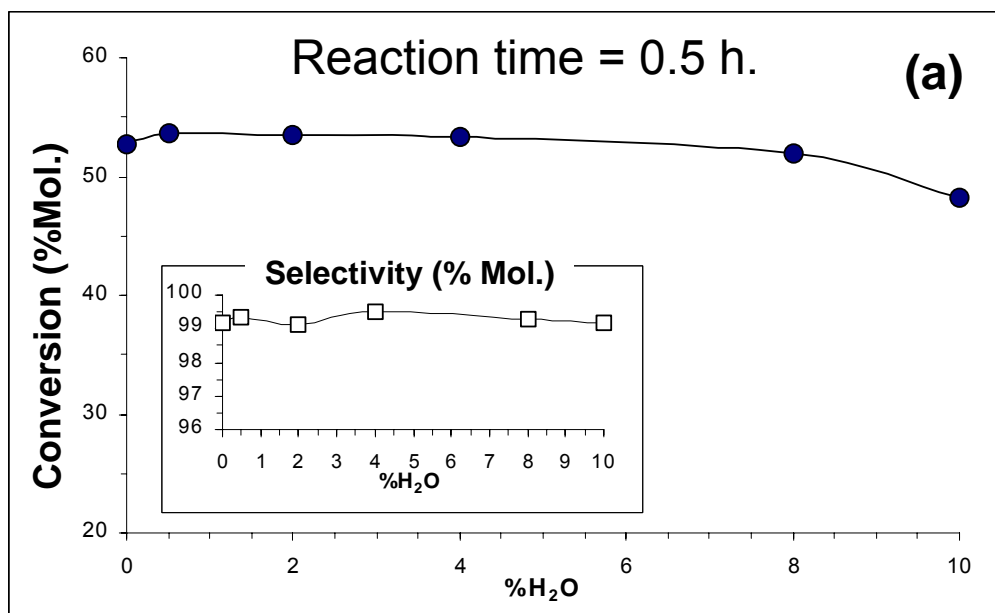
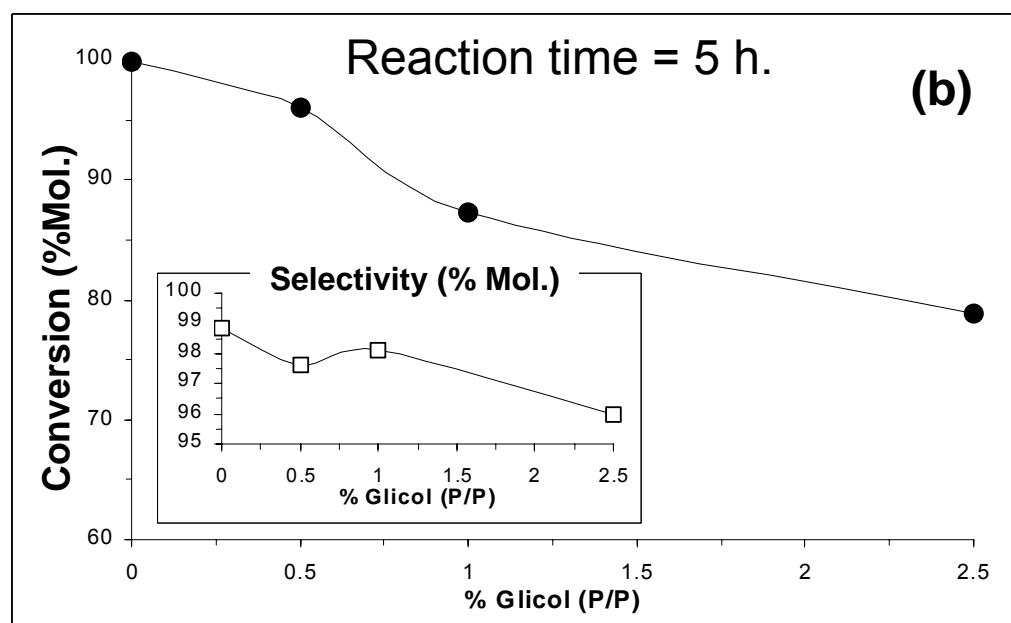
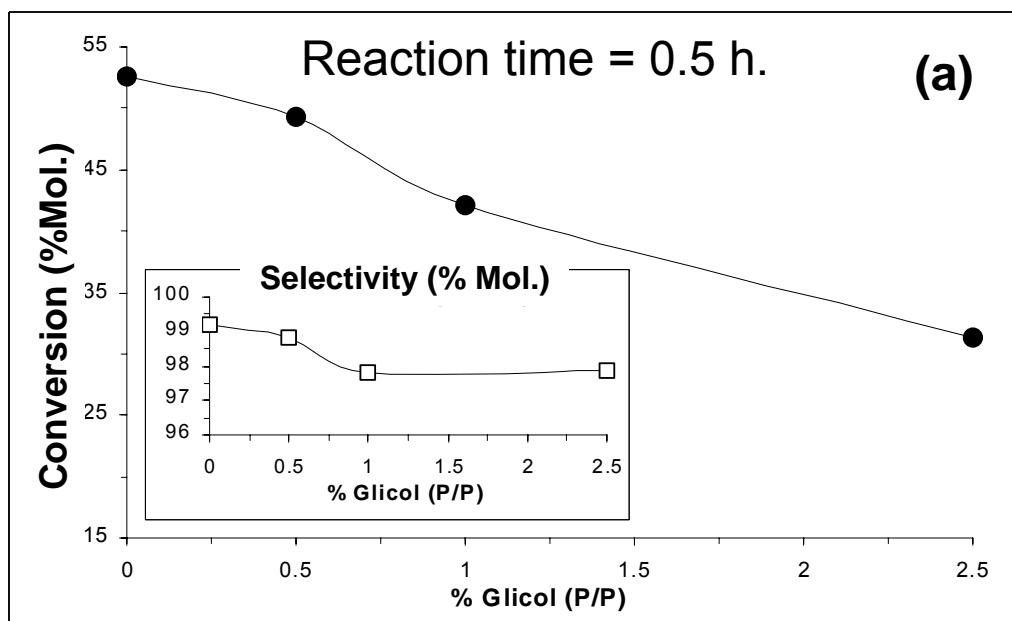
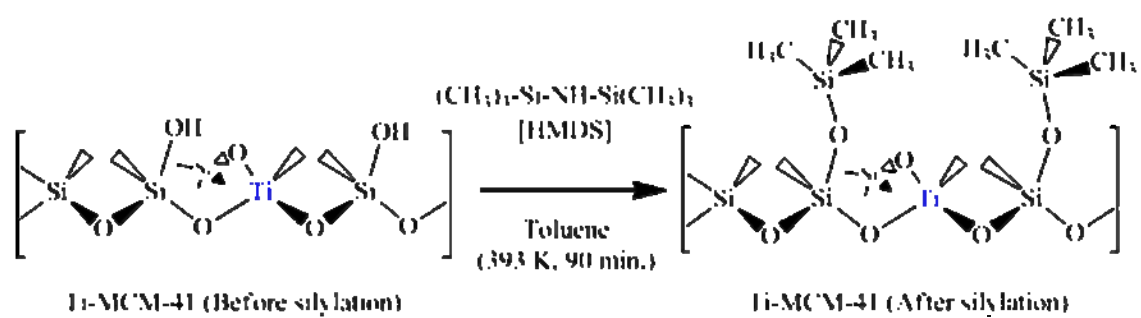


Figure 12:



Scheme 1



Tables**Table 1.** Physical and textural properties of Ti-MCM-41 materials with different silylation degrees.

Sample [wt% of C]	Material Composition (wt%) ^a			Surf. Area (m ² ·g ⁻¹) ^b	Pore Diam. (Å) ^c
	C content	N content	H content		
Ti-MCM-41[0.0]	0.00	---	0.68	1090	43
Ti-MCM-41[1.7]	1.69	0.07	0.98	1062	41
Ti-MCM-41[2.7]	2.77	0.08	1.02	1000	35
Ti-MCM-41[4.5]	4.50	0.06	1.47	964	34
Ti-MCM-41[6.0]	6.00	0.06	1.87	920	34
Ti-MCM-41[7.4]	7.40	0.07	2.04	869	34
Ti-MCM-41[8.9]	8.95	0.00	1.94	797	33

a- Determined by elemental analysis.- b- Calculated from the N₂ isotherm absorption measurements (BET method).- c- Calculated from the Ar isotherm absorption measurements by resolution of the Horvath-Karvazoe equation.-

Table 2. Areal enthalpies of immersion (mJ/m^2) into H_2O , cyclohexane, methanol, *tert*-butanol and acetonitrile for different silylated Ti-MCM-41 samples

C content (wt.%)	$-\Delta H_{\text{imm}}$ (mJ/m^2)				
	H_2O	Ciclohexane	Metanol	Tert-butanol	Acetonitrile
0	125.2	46.2	142.8	120.3	113.4
1.69	115.5	46.0	134.1	115.0	----
2.77	107.0	45.1	126.0	101.2	106.2
4.5	89.3	42.2	105.7	----	----
6	2.4	38.5	76.0	61.4	63.3
7.38	0	37.5	57.6	40.3	44.6
8.95	0	37.1	49.8	36.5	----

Table 3. Selective epoxidation of terpenes over Ti-MCM-41 calcined and silylated materials with TBHP at 343 K during 8 hours.^a

Terpene	Catalizador	Conversion (%Mol.)		Selectivity (%Mol.)		
		Terpene	TBHP	TBHP	Epoxide ^b	Others
Terpinolene	Ti-MCM-41[0.0]	43	54	66	35	65
	Ti-MCM-41 Silylated ^c	88	96	59	48	52
Limonene	Ti-MCM-41[0.0]	56	96	39	76	24
	Ti-MCM-41 Silylated ^c	93	96	67	73	27
α -pinene	Ti-MCM-41[0.0]	10	35	30	8	92
	Ti-MCM-41 Silylated ^c	85	90	98	78	22
α -cedrene	Ti-MCM-41[0.0]	22	44	41	60	40
	Ti-MCM-41 Silylated ^c	75	81	69	86	14

a- Reaction conditions: 8.5 mmol. of terpene, 10 mmol of TBHP, 150 mg of catalyst (≈ 2.0 wt% of TiO₂ on catalyst).- b- In the cases of limonene and terpinolene, Epoxide = cyclic epoxide + exo-cyclic epoxide.- c- Ti-MCM-41 Silylated [8.9 wt% of C content] = Ti-MCM-41[8.9].-